

# Emergence of foams from the breakdown of the phase field crystal model

Nicholas Guttenberg<sup>1</sup>, Nigel Goldenfeld<sup>1</sup> and Jonathan Dantzig<sup>2</sup>

<sup>1</sup>*Department of Physics, 1110 West Green Street,*

<sup>2</sup>*Department of Mechanical science and Engineering, 1206 West Green Street,  
University of Illinois at Urbana-Champaign, Urbana, Illinois, 61801-3080.*

The phase field crystal (PFC) model captures the elastic and topological properties of crystals with a single scalar field at small undercooling. At large undercooling, new foam-like behavior emerges. We characterize this foam phase of the PFC equation and propose a modified PFC equation that may be used for the simulation of foam dynamics. This minimal model reproduces von Neumann's rule for two-dimensional dry foams, and Lifshitz-Slyozov coarsening for wet foams. We also measure the coordination number distribution and find that its second moment is larger than previously-reported experimental and theoretical studies of soap froths, a finding that we attribute to the wetness of the foam increasing with time.

PACS numbers: 47.57.Bc, 64.70.D-, 47.54.-r

Computational modeling of large-scale systems usually involves either detailed molecular dynamics simulations, in which every particle must be tracked, or a highly coarse-grained model in which the underlying symmetries are known and are used to derive a continuum model from the underlying physics. Molecular dynamics is limited to small systems and/or to very short times, and coarse-grained models tend to fail at places where the underlying symmetries are broken, such as at defects and dislocations. The phase field crystal (PFC) model [1] is an intermediate approach with the advantage of diffusive time scale, but with atomic scale resolution of molecular dynamics. The PFC model can be used to capture the dynamics of defects and dislocations in large crystals [2, 3], the dynamics of grain interactions [4], molecular dynamics of vacancies [5] and even nonlinear elasticity [6]. In addition, it is amenable to methods such as coarse-graining and adaptive mesh refinement [7].

The dimensionless phase field crystal equation [1]

$$\frac{\partial \psi}{\partial t} = \nabla^2 [(\nabla^2 + 1)^2 \psi + r\psi + \psi^3] \quad (1)$$

is a density functional theory [2], best thought of as arising from phenomenological and symmetry considerations. In particular, this is the simplest class of models appropriate for systems whose dynamics is governed by minimizing departures from periodicity [8], as opposed to the situation in other materials processes, such as spinodal decomposition, where the dynamics minimizes departures from spatial uniformity. In principle this approach only holds for small values of the undercooling  $\alpha \equiv -r$ , beyond which the strong nonlinearity may in principle overwhelm the crystal's symmetries, leading to such artifacts as merger or dissolution of the 'atoms' of the model.

In this Rapid Communication, we explore an interesting feature of the phase field crystal model in the limit of large undercooling, which we show turns out to facilitate a simple, scalar and minimal model of foams. In the

appropriate density regimes, the behavior of the phase field crystal equation at large undercoolings is that the atoms of the crystal lattice begin to merge. However, the interstitial spaces between the atoms are preserved and become line solitons. The result is a coarsening foam-like structure. We analyze the process by which this instability in the equation of motion occurs, and use this understanding to propose a minimal, modified PFC model that is capable of describing quantitatively both wet and dry foams at the level of a continuum, scalar theory that is computationally efficient.

*Equilibrium Phase Diagram:-* The phase diagram of the PFC model has been computed for small undercoolings [1]. We shall use the same methods to construct the phase diagram at larger values of the undercooling in order to see what may be found there. First, however, we will convert the PFC equation and PFC energy to a nondimensionalized form with respect to the equilibrium liquid (constant phase) density. The energy minimizing density for the constant phase is  $\psi = \pm \sqrt{\alpha}$ , so we will introduce a nondimensional order parameter  $\phi \equiv \psi / \sqrt{\alpha}$ . This gives us the following free energy:

$$F = \int_V \frac{1}{2} \phi (\nabla^2 + 1)^2 \phi + \alpha \left( -\frac{1}{2} \phi^2 + \frac{1}{4} \phi^4 \right) dV \quad (2)$$

and corresponding equation of motion:

$$\frac{\partial \phi}{\partial t} = \nabla^2 ((\nabla^2 + 1)^2 \phi + \alpha(-\phi + \phi^3)) \quad (3)$$

We then construct the phase diagram at large  $\alpha$  by calculating the energy minima of the one-mode approximations for the constant phases  $L_{\pm} : \phi = \phi_0$ , where the subscript  $\pm$  refers to the sign of the average density  $\phi_0$ ; the striped phase  $S : \phi = \phi_0 + A_S \cos(x)$ , where  $A_S = \sqrt{\alpha(4 - 3\phi_0^2)}/3$ ; and the two triangular lattices  $\Delta_{\pm} : \phi = \phi_0 + (A_{\Delta} \pm B_{\Delta})(\cos(\vec{k}_1 \cdot \vec{r}) + \cos(\vec{k}_2 \cdot \vec{r}) + \cos(\vec{k}_3 \cdot \vec{r}))$ , where the  $\vec{k}_j$  are the lattice vectors of the regular triangular lattice,  $A_{\Delta} = -\alpha\phi_0/5$  and  $B_{\Delta} = \sqrt{\alpha(15 - 36\phi_0^2)}/15$ .

Even though the one-mode approximation is not accurate at these large values of  $\alpha$ , we use this approximation to understand heuristically the behavior observed, thus motivating our form for the modified phase field crystal model introduced below. Our main results, for the modified phase field crystal model, are fully time-dependent and independent of this approximation.

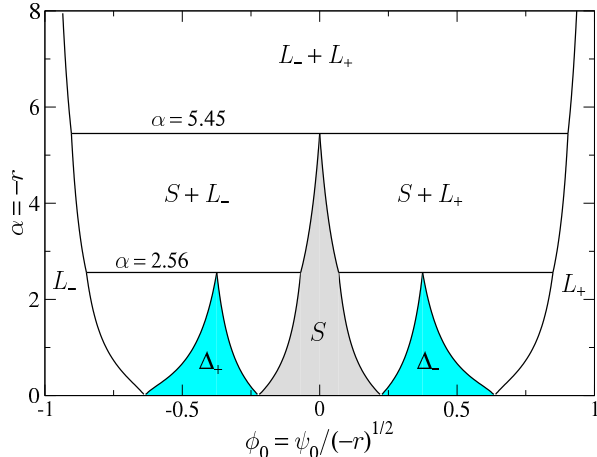


FIG. 1: (Color online). Phase diagram associated with the free energy in Eq. (2). Invariant reactions occur at  $\alpha = 2.56$  and  $\alpha = 5.45$ . No further topological changes occur for  $\alpha > 8$ .

The equilibrium phase diagram is obtained by substituting the various ansatz into Eqn. (3) and performing a common tangent construction. The result is shown in Fig 1. We find a series of previously undiscovered invariant points as  $\alpha$  increases. At  $\alpha = 2.56$ , the coexistence region between the striped and triangular phases disappears, giving rise to a coexistence between stripes and one of the liquid phases. Then, at  $\alpha = 5.45$  the striped phase vanishes, leaving only a region of immiscible liquid-liquid coexistence, and the regions comprised entirely of the liquid phases.

This can be understood by considering the influence of the two terms in the free energy. At small  $\alpha$ , the wavelength selection term that was added to construct the PFC equation is dominant. As  $\alpha$  increases, the local term that drives  $\phi$  to have the values of  $\pm 1$  becomes dominant, so that eventually the wavelength selection term  $(1 + \nabla^2)^2 \phi$  is a small perturbation and the equilibrium phases are determined by the average value of  $\phi_0^2/2 - \phi_0^4/4$ , which is minimized by the constant phases.

*Dynamics:-* The phase diagram we have just computed represents the behavior of this system in its final equilibrium state. However, the approach toward that equilibrium changes as  $\alpha$  increases. Starting from a hexagonal lattice, the system attempts to coarsen into two regions, one composed of  $L_+$ , the other composed of  $L_-$ . However, because of the small residual wavelength selection, there is a finite energy cost to removing spatially patterned structures. The consequence of this is that the

PFC ‘atoms’ are dynamically conserved by this infinitesimal energy barrier, which halts the coarsening dynamics. If the average density of the system is shifted, e.g., by deliberately reducing  $\phi_0$  over time, this can provide enough energy to destabilize the PFC atoms, but stripe-like cell walls will still remain stable for a longer period as they can move perpendicular to their length to create large bubbles of one of the liquids.

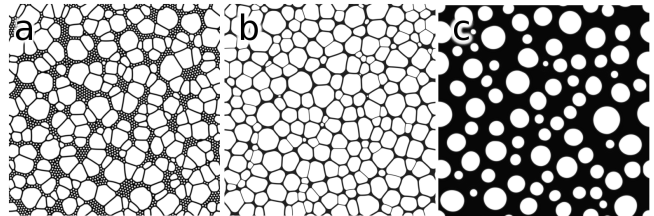


FIG. 2: a. Final state obtained from Eqn. (3) with  $\alpha = 16$  and  $\phi_0 = -0.41$  after coarsening. Residual atoms coexist with large foam cell regions. b. Simulation using the modified PFC equation for  $\alpha = 20$ , quenched with  $\phi_0 = 0.4$  initially, and then drained to  $\phi_0 = -0.6$ . The result is a dry foam structure with no residual atoms. c. Simulation of the modified PFC equation for  $\alpha = 20$  and  $\phi_0 = 0.25$ , allowed to coarsen without draining. The result is a wet foam structure with circular bubbles.

The end result of this is that a foam-like state appears (Fig 2a), which coarsens to a stationary point at which there are no more free adjustments that can be made to approach the equilibrium state. Thus, even a small perturbative addition of wavelength selection is sufficient to stabilize a foam-like structure.

Although this behavior is interesting from the point of view of understanding the properties of the phase field crystal model, it does not behave like a physical foam. The arrested coarsening and inability to get rid of residual atoms prevent this from being used as a model for studying coarsening foams. We now alter the free energy so as to destabilize the residual atoms while retaining the overall cellular structure, so that we may recover physical foam dynamics.

In effect what we wish to do is to weaken the wavelength selection while encouraging  $k = 0$  structures. A stripe has one  $k = 0$  direction and one direction with the selected wavelength, whereas an atom has two directions with the selected wavelength. If the selected wavelength sits at a local energy minimum, but the global minimum is at  $k = 0$ , then this should help remove residual atoms in favor of bubble interfaces.

The PFC wavelength selection operator  $(\nabla^2 + 1)^2$  corresponds in  $k$ -space to

$$E(k) = (1 - k^2)^2 \quad (4)$$

We modify this by introducing two parameters  $k_0$  and  $b$

$$E_{mod}(k) = (k/k_0)^2 (1 - (k/k_0)^2)^2 + b(k/k_0)^2 \quad (5)$$

and then choose  $k_0$  so as to retain minima at  $k = \pm 1$ :  $k_0 = [3/(2 + \sqrt{1 - 3b})]^{1/2}$ . The modified form of the free energy in real space becomes

$$F_{mod} = \int_V \frac{1}{2} \phi \left( \frac{1}{k_0^2} \nabla^2 \left( \frac{1}{k_0^2} \nabla^2 + 1 \right)^2 - \frac{b}{k_0^2} \nabla^2 \right) \phi + \alpha \left( -\frac{1}{2} \phi^2 + \frac{1}{4} \phi^4 \right) dV \quad (6)$$

We can then vary  $b$  to control the relative depths of the minima at  $k = \pm 1$ . The most extreme effect is achieved at  $b = -1/3$ , at which the minima at  $k = \pm 1$  disappear. We use this value of  $b$  throughout the rest of this paper.

The dynamics of the modified PFC equation give rise to the structures shown in Figs. 2b and 2c. If the system is quenched from a disordered state, one recovers Lifshitz-Slyozov coarsening dynamics [9] corresponding to the physical behavior of a very wet foam. On the other hand, if the system is drained from a state with positive average density to one with negative average density, polygonal cell walls form and coarsen by topological rearrangements.

*Results:-* We measured the coarsening dynamics and statistics of the eventual scaling state of the modified PFC equation in order to compare with physical foams. In order to measure the coarsening we are interested in the quantity  $\langle r \rangle(t)$ , the average bubble radius. We may easily count the total number of bubbles and so determine the average bubble area as  $\langle A \rangle(t) = A_{total}/N(t)$ . If we assume that deviations from circular geometry are small, then we may approximate  $\langle r \rangle(t) \approx \sqrt{\langle A \rangle(t)}$ .

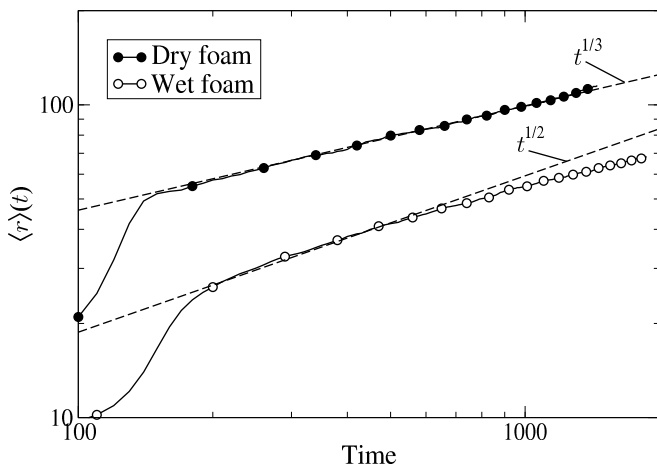


FIG. 3: Coarsening behavior of wet and dry foams in the modified PFC equation with  $\alpha = 20$ , compared with the corresponding theoretical coarsening laws.

For a wet foam, we expect the bubble growth to proceed as diffusive grain growth, so that  $\langle r \rangle(t) \propto t^{1/3}$ . As an example, we simulate a  $1024 \times 1024$  system with  $\alpha = 20$  and quench into an average density  $\phi_0 = 0.25$ . We ob-

serve a scaling  $\langle r \rangle \propto t^{0.34}$  (Fig 3, filled circles), consistent with the predicted growth law.

For a dry foam in two dimensions, von Neumann's law for bubble area growth [10] is

$$\frac{dA}{dt} = \kappa(n - 6) \quad (7)$$

where  $\kappa$  is an effective diffusivity, and  $n$  is the coordination number of the bubble. This implies that the average bubble radius should scale as  $\langle r \rangle(t) \propto t^{1/2}$ . To measure the coarsening of a dry foam, we quench from an average density  $\phi_0 = 0.3$  and drain slowly to a density of  $\phi_0 = -0.4$ . We start measuring the coarsening dynamics after we have stopped draining. However, our reference point for  $t = 0$  is still the point of the quench. We observe a scaling  $r \propto t^{0.43}$ , significantly slower than the predictions of von Neumann's law (Fig 3, open circles). At late times in the simulation, the bubble interfaces start to become wet. If we restrict our analysis to times shortly after coarsening begins, the resulting fit exponent increases to  $r \propto t^{0.47}$ . This indicates that we are probably seeing the effect of not having a fully dry foam at any point in time.

As two-dimensional froths coarsen, they are expected to reach a self-similar scaling state in which the normalized moments of the distribution of areas and of coordination number are expected to become time independent. The second moment of the coordination number distribution has been used as a probe of this scaling state. Glazier and Weaire [11] predict that the coordination number distribution should eventually reach a universal limiting scaling state with a second moment  $\mu_2 = 1.4$ , with a strongly non-monotonic transient behavior.

We measure the coordination number distribution of the dry foam by a watershed algorithm. [12] We superimpose a grid over the system and fill each bubble with a unique integer. We then allow these integers to propagate to neighboring unoccupied cells, and then find the total number of different integers that a given bubble comes into contact with. We observe a similar time-dependence of the second moment of our distribution, but the measured limiting value  $\mu_2 = 2.31 \pm 0.01$  is significantly different from 1.4 (see Fig 4). In other models and simulations of coarsening 2D foams, the observed limiting value of  $\mu_2$  has been variously reported as 1.9 [13], and 1.7 [14], and 1.5 [15], and experiments have measured from 1.4 [16] in soap froths to values as small as 0.14 and 0.22 in magnetic froths [17].

We conclude that the second moment is either not a universal quantity, or else that there are strong transients which make any universal scaling regime difficult to observe in practice. We note that our foam is not completely dry, and that the absence of a drainage mechanism implies that the foams becomes wetter the more they coarsen. Whether real foams undergo a corresponding change of regime is not clear.

We have found that in the limit of large undercooling,

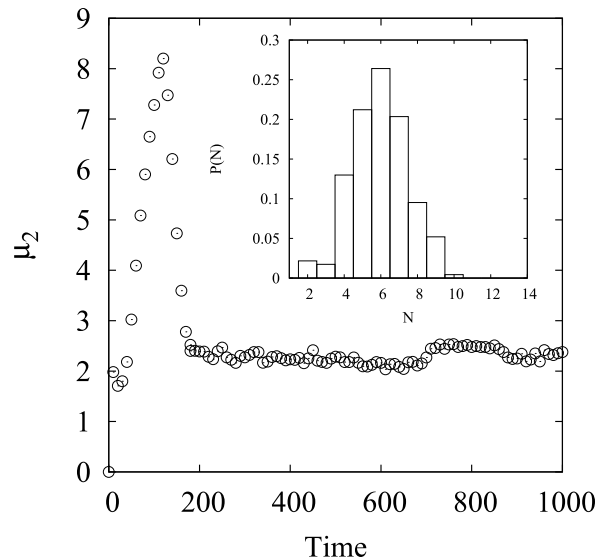


FIG. 4: Evolution of the second moment of the bubble coordination number in a dry foam realized by the modified PFC equation. The bubble distribution broadens during the transition to power-law coarsening, after which it reduces to a steady value of  $2.31 \pm 0.01$ . The inset shows a particular distribution at  $t = 1800$ .

the phase field crystal equation produces topologically stabilized foams. These foams are a consequence of the residual wavelength selection, which acts as a singular perturbation that prevents the destruction of cell walls and forces the coarsening to take place via topological rearrangements. The fact that this behavior emerges from a minimal model such as the phase field crystal equation suggests a general mechanism by which foams may occur in natural systems.

The ingredients of the phase field crystal equation are a driving force towards certain equilibrium densities, some sort of spatial relaxation (diffusion, viscosity, and the like), and some competing source of wavelength selection. Such a system, in the limit where the wavelength selection is weak compared to the other forces, would likely give rise to a foam. This mathematical structure can be seen in models of magnetic froths [17], Type-I superconductors [18], and in models of polygonal cells found in melting snow [19].

However, the foams produced in this limit of the PFC equation have unphysical properties. The wavelength selection also preserves atoms: bubbles whose diameter is comparable to the width of the cell walls. This can be ameliorated by modifying the PFC free energy to penalizes atoms while encouraging stripes. As a result, the coarsening dynamics of real foams are recovered although the distribution of bubbles in the resultant scaling state

appears to be somewhat different.

If these differences are understood, the modified PFC equation may be a useful tool in modelling foams, as it is simpler than other existing methods such as Q-Potts models [20] and minimal surface evolution [21], and is fairly easy to simulate, having only one field and a spatial structure that is easily treated with spectral methods.

We are grateful to B. Athreya for discussions about the stability of the PFC equation. N. Guttenberg was supported by a University of Illinois Distinguished Fellowship, and J. Dantzig acknowledges the support of the US Dept. of Energy, under subcontract 4000076535.

- 
- [1] K. Elder and M. Grant, *Physical Review E* **70**, 051605 (2004).
  - [2] K. Elder, N. Provatas, J. Berry, P. Stefanovic, and M. Grant, *Physical Review B* **75**, 064107 (2007).
  - [3] N. Provatas, J. Dantzig, B. Athreya, P. Chan, P. Stefanovic, N. Goldenfeld, and K. Elder, *JOM Journal of the Minerals, Metals and Materials Society* **59**, 83 (2007).
  - [4] J. Mellenthin, A. Karma, and M. Plapp, *Physical Review B* **78**, 184110 (2008).
  - [5] P. Chan, N. Goldenfeld, and J. Dantzig, *Physical Review E* **79**, 035701(R) (2009).
  - [6] P. Y. Chan and N. Goldenfeld, *Phys. Rev. E* **80**, 065105(R) (2009).
  - [7] N. Goldenfeld, B. Athreya, and J. Dantzig, *Physical Review E* **72**, 020601(R) (2005).
  - [8] S. A. Brazovskii, *Zh. Eksp. Teor. Fiz.* **68**, 175 (1975).
  - [9] A. Bray, *Advances in Physics* **51**, 481 (2002).
  - [10] J. Von Neumann, *American Society for Testing Materials*, Cleveland **108** (1952).
  - [11] J. Glazier and D. Weaire, *Journal of Physics: Condensed Matter* **4**, 1867 (1992).
  - [12] F. Meyer, in *8me congrès de reconnaissance des formes et intelligence artificielle* (1991), vol. 2, pp. 847–857.
  - [13] M. Marder, *Physical Review A* **36**, 438 (1987).
  - [14] H. Flyvbjerg, *Physical Review E* **47**, 4037 (1993).
  - [15] J. Glazier, M. Anderson, and G. Grest, *Philosophical Magazine. Pt. B. Structural, Electronic, Optical and Magnetic Properties* **62**, 615 (1990).
  - [16] J. Stavans and J. Glazier, *Physical Review Letters* **62**, 1318 (1989).
  - [17] F. Elias, C. Flament, J. Bacri, O. Cardoso, and F. Graner, *Physical Review E* **56**, 3310 (1997).
  - [18] R. Prozorov, A. Fidler, J. Hoberg, and P. Canfield, *Nature Physics* **4**, 327 (2008).
  - [19] T. Tiedje, K. Mitchell, B. Lau, A. Ballestad, and E. Nodwell, *J. of Geophys. Res* **111**, F02015 (2006).
  - [20] Y. Jiang and J. Glazier, *Philosophical Magazine Letters* **74**, 119 (1996).
  - [21] R. Phelan, D. Weaire, and K. Brakke, *Experimental Mathematics* **4**, 181 (1995).